Deletion of *Mthfd1l* causes embryonic lethality and neural tube and craniofacial defects in mice

Jessica Momb[a], Jordan P. Lewandowski[b,c], Joshua D. Bryant[a], Rebecca Fitch[d], Deborah R. Surman[b], Steven A. Vokes[b,c], and Dean R. Appling[a,b,1]

[a]Department of Chemistry and Biochemistry, [b]Institute for Cellular and Molecular Biology, [c]Section of Molecular Cell and Developmental Biology, and [d]Dell Pediatric Research Institute, The University of Texas at Austin, Austin, TX 78712

Edited by David W. Russell, University of Texas Southwestern Medical Center, Dallas, TX, and approved November 30, 2012 (received for review July 3, 2012)

Maternal supplementation with folic acid is known to reduce the incidence of neural tube defects (NTDs) by as much as 70%. Despite the strong clinical link between folate and NTDs, the biochemical mechanisms through which folic acid acts during neural tube development remain undefined. The *Mthfd1l* gene encodes a mitochondrial monofunctional 10-formyl-tetrahydrofolate synthetase, termed MTHFD1L. This gene is expressed in adults and at all stages of mammalian embryogenesis with localized regions of higher expression along the neural tube, developing brain, craniofacial structures, limb buds, and tail bud. In both embryos and adults, MTHFD1L catalyzes the last step in the flow of one-carbon units from mitochondria to cytoplasm, producing formate from 10-formyl-THF. To investigate the role of mitochondrial formate production during embryonic development, we have analyzed *Mthfd1l* knockout mice. All embryos lacking *Mthfd1l* exhibit aberrant neural tube closure including craniorachischisis and exencephaly and/or a wavy neural tube. This fully penetrant folate-pathway mouse model does not require feeding a folate-deficient diet to cause this phenotype. Maternal supplementation with sodium formate decreases the incidence of NTDs and partially rescues the growth defect in embryos lacking *Mthfd1l*. These results reveal the critical role of mitochondrially derived formate in mammalian development, providing a mechanistic link between folic acid and NTDs. In light of previous studies linking a common splice variant in the human *MTHFD1L* gene with increased risk for NTDs, this mouse model provides a powerful system to help elucidate the specific metabolic mechanisms that underlie folate-associated birth defects, including NTDs.

Closure of the neural tube during development is a highly complex but poorly understood process. Not surprisingly, neural tube defects (NTDs) have a multifactorial etiology, including both genetic and environmental factors. The importance of maternal folate status to NTD risk was first suggested more than 40 y ago (1). Many human studies show that periconceptional intake of supplemental folic acid can reduce the incidence of NTDs by as much as 70% in some populations (reviewed in ref. 2). These results led to mandated fortification of all enriched cereal grain products with folic acid in the United States beginning in 1996 to ensure that women of child-bearing age would consume adequate quantities of the vitamin. Although folic acid fortification has decreased NTD incidence in some subpopulations, fortification has not completely eliminated NTDs (3). Despite the strong clinical link between folate and NTDs, the biochemical mechanisms through which folic acid acts during neural tube development remain undefined.

Folate-dependent one-carbon (1C) metabolism is highly compartmentalized in eukaryotes, and mitochondria play a critical role in cellular 1C metabolism (4). The cytoplasmic and mitochondrial compartments are metabolically connected by transport of 1C donors such as serine, glycine, and formate across the mitochondrial membranes, supporting a mostly unidirectional flow (clockwise in Fig. 1) of 1C units from serine to formate, and onto purines, thymidylate (dTMP), and methionine. It appears that under most conditions, the majority of 1C units for cytoplasmic processes are derived from mitochondrial formate (reviewed in ref. 4). This formate is exported to the cytoplasm where it is reattached to tetrahydrofolate (THF) for use in de novo purine biosynthesis, or further reduced for either thymidylate synthesis or remethylation of homocysteine to methionine. The 1C unit interconverting activities represented in Fig. 1 by reactions 1–3 (and 1m–3m in mitochondria) are the central players in this intercompartmental pathway. These crucial reactions are catalyzed by members of the methylenetetrahydrofolate dehydrogenase (MTHFD) family in eukaryotes. The first member of this family to be characterized was the cytoplasmic MTHFD1 protein, a trifunctional enzyme possessing 10-formyl-THF synthetase, 5,10-methenyl-THF cyclohydrolase, and 5,10-methylene-THF dehydrogenase activities (reactions 1–3). This enzyme incorporates formate, released from mitochondria, into the cytoplasmic 1C THF pool as 10-formyl-THF (CHO-THF), which is required for de novo purine biosynthesis. MTHFD1 can also catalyze reduction of the 1C unit to 5,10-methylene-THF (CH_2-THF) for dTMP synthesis (reaction 10), or for methyl group biogenesis via 5-methyl-THF (CH_3-THF) (reaction 6).

Identification of the enzymes that catalyze reactions 1m–3m in mammalian mitochondria has lagged behind that of the cytoplasmic portion of the pathway. The MTHFD2 protein is a mitochondrial bifunctional CH_2-THF dehydrogenase/methenyl-THF cyclohydrolase (reactions 3m and 2m) (5). However, because MTHFD2 is expressed only in transformed mammalian cells and embryonic or nondifferentiated tissues (6) the enzyme(s) responsible for the CH_2-THF dehydrogenase/methenyl-THF cyclohydrolase activities observed in adult mammalian mitochondria (7) remained unknown. This gap was recently filled by identification of a new mitochondrial CH_2-THF dehydrogenase isozyme, encoded by the *Mthfd2l* gene, expressed in embryos and in adult tissues (8). Like MTHFD2, the MTHFD2L enzyme is bifunctional, possessing both CH_2-THF dehydrogenase and methenyl-THF cyclohydrolase activities (reactions 3m and 2m).

The final step in the mammalian mitochondrial pathway to formate (reaction 1m) is catalyzed by mitochondrial 10-formyl-THF synthetase, encoded by the *Mthfd1l* gene (9). Despite sharing 61% amino acid similarity with the cytoplasmic trifunctional MTHFD1, MTHFD1L is a monofunctional enzyme, possessing only the 10-formyl-THF synthetase activity (reaction 1m) (10). The *Mthfd1l* gene is expressed in most adult tissues, but at higher levels in spleen, thymus, brain, and placenta (9, 11). The *Mthfd1l* gene is also expressed at all stages of mammalian embryogenesis and ubiquitously throughout the embryo but with localized regions of higher expression along the neural tube, the brain, craniofacial structures, limb buds, and the tail bud (12). Moreover, metabolic tracer experiments in mouse embryonic fibroblasts showed that more than 75% of 1C units that enter the cytoplasmic methyl cycle are mitochondrially derived (12). Thus, in both embryos and adults, MTHFD1L catalyzes production of

Author contributions: J.M., J.P.L., S.A.V., and D.R.A. designed research; J.M., J.P.L., J.D.B., R.F., and D.R.S. performed research; J.M., J.P.L., S.A.V., and D.R.A. analyzed data; and J.M., J.P.L., S.A.V., and D.R.A. wrote the paper.

The authors declare no conflict of interest.

This article is a PNAS Direct Submission.

[1]To whom correspondence should be addressed. E-mail: dappling@austin.utexas.edu.

This article contains supporting information online at www.pnas.org/lookup/suppl/doi:10.1073/pnas.1211199110/-/DCSupplemental.

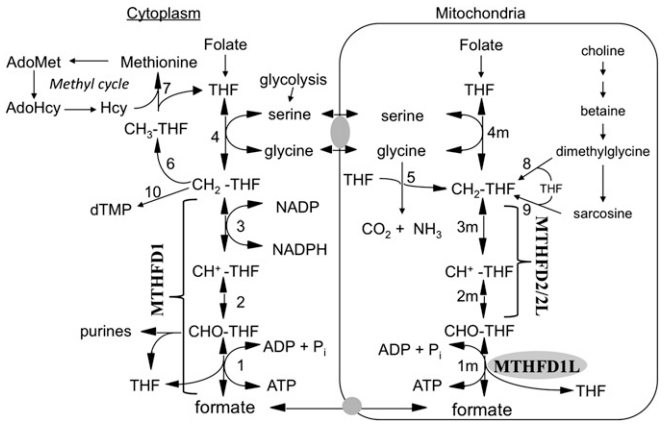

Fig. 1. Mammalian one-carbon metabolism. Reactions 1–4 are in both the cytoplasmic and mitochondrial (m) compartments. Reactions 1, 2, and 3, 10-formyl-THF synthetase, 5,10-methenyl-THF cyclohydrolase, and 5,10-methylene-THF dehydrogenase, respectively, are catalyzed by trifunctional C_1-THF synthase (MTHFD1) in the cytoplasm. In mammalian mitochondria, reaction 1m is catalyzed by monofunctional MTHFD1L and reactions 2m and 3m by bifunctional MTHFD2 or MTHFD2L. The other reactions are catalyzed by the following: 4 and 4m, serine hydroxymethyltransferase (SHMT); 5, glycine cleavage system (GCS); 6, 5,10-methylene-THF reductase; 7, methionine synthase; 8, dimethylglycine dehydrogenase; 9, sarcosine dehydrogenase; and 10, thymidylate synthase. All reactions from choline to sarcosine are mitochondrial except the betaine to dimethylglycine conversion, which is cytoplasmic. Hcy, homocysteine; AdoHcy, S-adenosylhomocysteine; AdoMet, S-adenosylmethionine.

formate from 10-formyl-THF, the last step in the flow of 1C units from mitochondria to cytoplasm.

To investigate the role of mitochondrial formate production during development, we have analyzed *Mthfd1l* knockout mice. We show here that loss of MTHFD1L is lethal to developing embryos, causing fetal growth restriction and aberrant neural tube closure with 100% penetrance in embryos that develop past the point of neural tube closure. Although there are other folate-related mouse models that exhibit NTDs, the *Mthfd1l* knockout mouse is a fully penetrant model that does not require feeding a folate-deficient diet to cause this phenotype. Moreover, we show that maternal supplementation with sodium formate decreases the incidence of NTDs and partially rescues the growth defect in embryos lacking *Mthfd1l*. These results reveal the critical role of mitochondrial formate in mammalian development, providing a mechanistic link between folic acid and neural tube defects. In light of previous studies linking a common splice variant in the human *MTHFD1L* gene with increased risk for NTDs (13), this mouse model provides a powerful system to help elucidate the specific metabolic mechanisms that underlie folate-associated birth defects, including NTDs.

Results

***Mthfd1l* Is Essential in Mice.** We obtained a strain of conditional knockout ready *Mthfd1l* mice from the European Conditional Mouse Mutagenesis Program (EUCOMM). In this strain, the *Mthfd1l* locus is modified by the insertion of a cassette, containing a splice acceptor, internal ribosome entry site, the β-galactosidase gene (*LacZ*) followed by a polyadenylation signal, and the gene for neomycin phosphotransferase (*Neo*) between exons 4 and 6 of *Mthfd1l* (Fig. 2*A*). This allele has three LoxP sites: one between the polyadenylation signal and *Neo* and two flanking exon 5. To generate a null allele, the mice were crossed to a Cre deleter strain, E2a-Cre (14). Recombination at the LoxP sites removes *Neo* and exon 5 to produce a disrupted allele containing *LacZ* followed by a polyadenylation signal (Fig. 2*A*). Transcription of the disrupted allele is expected to produce a transcript containing exons 1–4 spliced to *LacZ*. The disrupted *Mthfd1l* allele will herein be designated as $Mthfd1l^{z}$. The genotype was confirmed by PCR (Fig. 2*B*) and RT-PCR analysis indicated that the WT *Mthfd1l* transcript is absent in $Mthfd1l^{z/z}$ embryos (Fig. 2*C*). Full-length MTHFD1L protein is undetectable in $Mthfd1l^{z/z}$ embryos (Fig. 2*D*), indicating that this is a likely null allele. No difference in growth from weaning to 5 wk of age was observed between $Mthfd1l^{+/+}$ and $Mthfd1l^{z/+}$ mice. To determine the viability of homozygous null ($Mthfd1l^{z/z}$) mice, $Mthfd1l^{z/+}$ mice were intercrossed and the genotype distribution was determined (Table S1). A total of 172 weanlings from 31 litters were examined. The average litter size was 5.5 pups. The *Mthfd1l* genotypes were not distributed as expected for Mendelian inheritance of the nonfunctional $Mthfd1l^{z}$ allele. The ratio of $Mthfd1l^{+/+}$ to $Mthfd1l^{z/+}$ to $Mthfd1l^{z/z}$ was 55:117:0, indicating that the $Mthfd1l^{z/z}$ genotype causes embryonic lethality ($P = 2.0 \times 10^{-11}$). If it is assumed that the $Mthfd1l^{z/z}$ genotype is lethal, $Mthfd1l^{+/+}$ and $Mthfd1l^{z/+}$ genotypes were observed in the expected frequency ($P = 0.75$). Males and females were found at the expected frequencies, and $Mthfd1l^{z/+}$ mice appear healthy and breed normally.

Homozygous Deletion of *Mthfd1l* Results in Delayed Embryonic Growth and Defective Neural Tube Closure. Because we did not recover any $Mthfd1l^{z/z}$ pups at birth, we sought to determine the embryonic phenotype. Embryos were dissected from pregnant dams at E8.5–E15.5, genotyped using yolk sac tissue, and their gross morphology was examined. All observed $Mthfd1l^{z/z}$ embryos exhibited a growth delay compared with WT and $Mthfd1l^{z/+}$ littermates. The

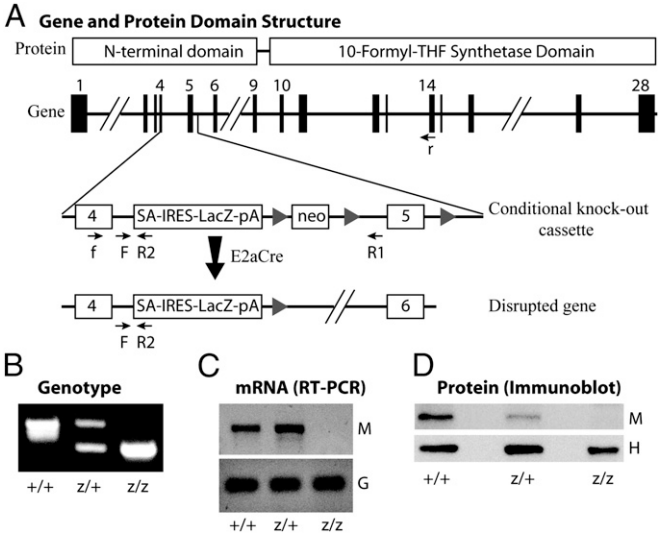

Fig. 2. $Mthfd1l^{z/z}$ embryos do not produce detectable protein or full-length transcripts. (*A*) The *Mthfd1l* gene, comprising 28 exons, encodes a protein with two domains. The catalytic domain begins in exon 10. Mice in which exon 5 was initially flanked by LoxP sites were crossed with the *E2a*-Cre line, producing offspring with complete recombination at the LoxP sites (gray arrowheads) and the resulting deletion of exon 5 and the *neomycin phosphotransferase* gene (*Neo*). Transcription from the endogenous *Mthfd1l* promoter produces a transcript containing exons 1–4 of *Mthfd1l* fused to an internal ribosome entry site (IRES) and the β-galactosidase gene (*LacZ*) followed by a polyadenylation site (pA). SA, splice acceptor site. (*B*) For genotyping, mouse genomic DNA was subjected to allele specific amplification using a mixture containing F, R1 and R2 primers (*Methods*). A genomic fragment of 444 bp was amplified from the WT allele and a 324-bp fragment was amplified from the $Mthfd1l^{z}$ allele. (*C*) RT-PCR analysis of mRNA expressed in whole E11.5 embryos using primers f in exon 4 and r in exon 14, yielding a 1,087-bp product. *M*, Mthfd1L; *G*, glyceraldehyde-3-phosphate dehydrogenase. (*D*) Immunoblot of mitochondria isolated from whole E11.5 embryos. Each lane was loaded with 7 μg of total mitochondrial protein. Blots were probed with antibodies against MTHFD1L (*M*, 100 KDa) or the mitochondrial matrix marker, Hsp60 (*H*, 60 KDa).

severity of the developmental delay was variable, but on average the null embryos appeared to lag ~0.75 d behind their littermates. Some of the *Mthfd1l*$^{z/z}$ embryos died early during the gestational period, but all that survived past the point of neural tube closure (E9.5) exhibited aberrant neural tube phenotypes. Of 152 embryos dissected between E11.5–E12.5, we obtained 52 *Mthfd1l*$^{+/+}$ embryos, 74 *Mthfd1l*$^{z/+}$ embryos, and 26 *Mthfd1l*$^{z/z}$ embryos, and we observed 28 resorptions. Of the 26 *Mthfd1l*$^{z/z}$ embryos, 15 exhibited a clear NTD phenotype (exencephaly or craniorachischisis) and 9 displayed a wavy neural tube phenotype (Fig. 3 *B–E*). The remaining two *Mthfd1l*$^{z/z}$ embryos had completely open neural tubes but were not scored as having craniorachischisis because these embryos had failed to turn, suggesting that they may have been in the process of resorption. The most common NTD phenotype was exencephaly with a wavy neural tube (Fig. 3*D*; $n = 11$), or exencephaly alone (Fig. 3*B*, $n = 3$). The most severe NTD observed was craniorachischisis (Fig. 3*C*; $n = 1$). The nine *Mthfd1l*$^{z/z}$ embryos whose neural tubes had closed all displayed a wavy neural tube with a small, aberrantly formed head (Fig. 4*B*). In all, 20/24 *Mthfd1l*$^{z/z}$ embryos exhibited a wavy neural tube, and the earliest observation of this phenotype was at E9.5. The location of the waviness in the neural tube was variable, but most embryos exhibited a wavy neural tube beginning at approximately the same axis as the forelimb and extending caudally past the forelimb, as depicted in Fig. 3 *D* and *E*. Because many studies have noted an increased incidence of NTDs in females (15), E11.5–E12.5 *Mthfd1l*$^{z/z}$ embryos were genotyped for presence of the sex-receptor Y (SRY) locus. No bias was found for either sex [females $n = 6$ (40%), males $n = 9$ (60%), $P = 0.44$].

In addition to aberrations in neural tube closure, we also noted facial deformities in *Mthfd1l*$^{z/z}$ embryos that were most apparent at the later stages. Compared with somite-matched WT or heterozygous embryos, E12.5 *Mthfd1l*$^{z/z}$ embryos display immature maxillary and mandibular processes (Fig. 3*G*). In *Mthfd1l*$^{z/z}$ embryos, the maxillary processes of the first branchial arch appear globular and more widely separated than in somite-matched control embryos. In addition, the mandibular processes are undergrown (Fig. 3 *F* and *G*; $n = 7/7$ embryos examined). No surviving *Mthfd1l*$^{z/z}$ embryos were observed after E12.5, preventing a later analysis of the phenotype.

Histological Analysis of Neural Tube Phenotypes. We sectioned control (*Mthfd1l*$^{z/+}$) and *Mthfd1l*$^{z/z}$ embryos stained for β-galactosidase at E10.5 and E11.5. This allowed us to visualize regionalized β-galactosidase activity, which should act as a reporter for *Mthfd1l* transcription (Fig. 2*A*). To confirm that the *LacZ* reporter recapitulated endogenous *Mthfd1l* gene expression, we compared the patterns detected by β-galactosidase staining in *Mthfd1l*$^{z/+}$ sections with endogenous *Mthfd1l* gene expression. Using in situ hybridization, we observed transcript expression in the ectoderm, underlying mesenchyme, and dorsal neural tube (Fig. 4 *C*, *F*, and *I*). In the neural tube, the highest expression is detected in the basal surface of the dorsal neuroepithelium (Fig. 4*F*, arrowheads). β-galactosidase activity was more restricted in *Mthfd1l*$^{z/+}$ embryos (Fig. 4*D*), but is still seen within the same region of the neural tube as the gene expression pattern. We conclude that the *LacZ* reporter partially recapitulates endogenous *Mthfd1l* gene expression with the difference most likely being due to reduced sensitivity.

Mthfd1l$^{z/+}$ whole mount embryos stained for β-galactosidase activity have the highest levels in the eyes, heart, limb, and dorsal midline region (Fig. 4 *A* and *J*). In sectioned *Mthfd1l*$^{z/+}$ embryos, β-galactosidase activity is predominantly detected at the basal surface of the dorsal neuroepithelium and is rarely detected in cells within and outside of the neural tube (Fig. 4 *D*, *G*, *L*, and *N*). In sectioned *Mthfd1l*$^{z/z}$ embryos, β-galactosidase activity is robustly detected both inside and outside the neural tube (Fig. 4 *E*, *H*, *M*, and *O*). Similar to *Mthfd1l*$^{z/+}$ embryos, β-galactosidase is detected in the neuroepithelium; however, expression is less restricted dorsally in the nulls. In *Mthfd1l*$^{z/z}$ embryos with closed neural tubes, the morphology was abnormal throughout the neural tube in all embryos sectioned (E10.5 and E11.5, $n = 6$). Neural tubes had abnormally shaped lumens, including asymmetric dorsal-lateral bulges as well as a broader dorsal lumen that were not seen in controls (Fig. 4 *D*, *E*, *G*, *H*, and *L–O*).

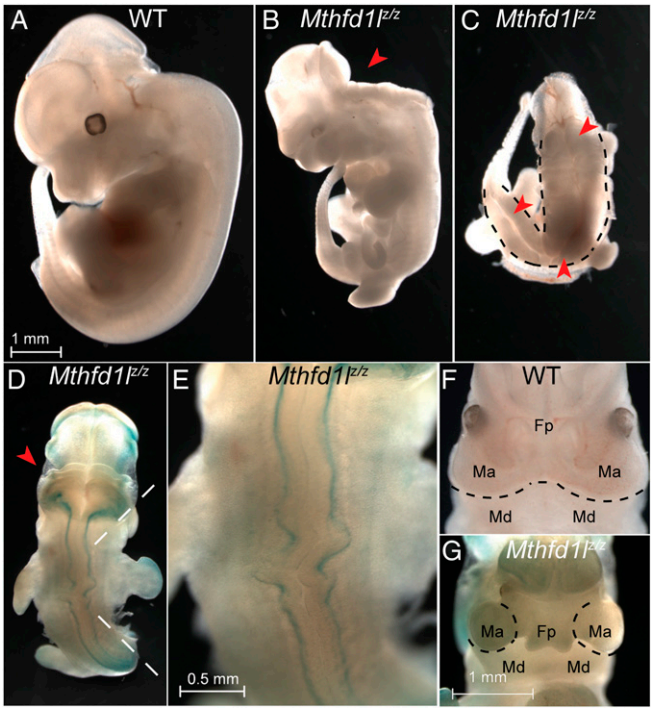

Fig. 3. *Mthfd1l*$^{z/z}$ embryos have neural tube and facial defects. Compared with WT E12.5 embryos (*A*), E12.5 *Mthfd1l*$^{z/z}$ embryos (*B–E*) exhibit a spectrum of neural tube defects including exencephaly (*B*, red arrowhead). (*C*) Embryo with completely open neural folds (craniorachischisis) is indicated by the dashed lines. Note that the embryo curves to the left so the entire open neural tube is visible (red arrowheads). (*D*) Embryo with exencephaly (red arrowhead) and a wavy neural tube. (Magnification: *E*, 3.2×.) (*F*) WT, 51-somite embryo showing normal facial development. (*G*) Same *Mthfd1l*$^{z/z}$ embryo (51 somites) imaged (*D* and *E*) displaying facial defects. The maxillary processes (Ma) are globular and are broadly separated from the midline (indicated by the frontonasal prominence, Fp). The mandibular processes (Md) in the *Mthfd1l*$^{z/z}$ embryo appear undergrown. Embryos (*D*, *E*, and *G*) are stained for β-galactosidase activity (blue). Embryos (*A–D*) are imaged at the same magnification (1.25×). Embryos (*F* and *G*) are at the same magnification (2×).

Dietary Supplementation with Sodium Formate. Because disruption of *Mthfd1l* is expected to result in loss of mitochondrial formate production, we sought to determine if maternal formate supplementation would improve development of *Mthfd1l*$^{z/z}$ embryos. Pregnant dams were given ad libitum access to water containing sodium formate to achieve a calculated dose of 5,000 or 7,500 mg sodium formate·kg^{-1}·d^{-1} (*Methods*); controls were given water without formate. As before, we did not recover *Mthfd1l*$^{z/z}$ embryos from unsupplemented dams (17 *Mthfd1l*$^{+/+}$, 34 *Mthfd1l*$^{z/+}$, and 0 *Mthfd1l*$^{z/z}$ embryos, deviating significantly from the expected Mendelian ratio; $P = 0.0002$). When dams were supplemented with 5,000 mg·kg^{-1}·d^{-1} sodium formate, we obtained 4 *Mthfd1l*$^{+/+}$, 14 *Mthfd1l*$^{z/+}$, and 8 *Mthfd1l*$^{z/z}$ embryos from three litters between E15.5–18.5. This genotype distribution does not differ significantly from the expected Mendelian ratio ($P = 0.50$), suggesting at least a partial rescue by formate. We next examined the morphology of E10.5–E15.5 embryos from dams supplemented with 7,500 mg·kg^{-1}·d^{-1} sodium formate, obtaining 10 *Mthfd1l*$^{+/+}$ embryos, 31 *Mthfd1l*$^{z/+}$ embryos, and 14 *Mthfd1l*$^{z/z}$ embryos from six litters, again conforming to the expected Mendelian ratio ($P = 0.48$). Of the 14 *Mthfd1l*$^{z/z}$ embryos, 11

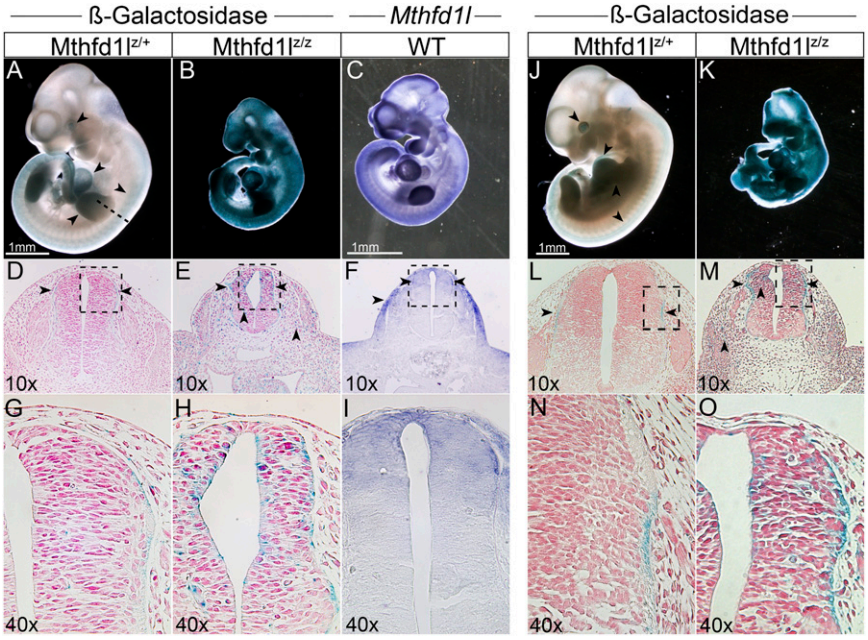

Fig. 4. Aberrant neural tube morphology in *Mthfd1l*$^{z/z}$ embryos. (*A* and *J*) *Mthfd1l*$^{z/+}$ embryos at approximately E10.5 and E11.5, respectively, exhibit regionalized β-galactosidase staining that is highest in the eyes, heart, limb, and dorsal midline region (black arrowheads). (*A*) Dashed line indicates the level of all sections below, at 10× and 40× magnification. (*B* and *K*) *Mthfd1l*$^{z/z}$ littermates of embryos in (*A*) and (*J*), respectively, exhibit β-galactosidase staining that appears superficially ubiquitous. (*D, G, L,* and *N*) Sections through *Mthfd1l*$^{z/+}$ embryos have β-galactosidase activity in the basal area of the dorsal neuroepithelium while *Mthfd1l*$^{z/z}$ embryos (*E, H, M,* and *O*) have a smaller neural tube, kinks in the lumen, and a broader dorsal lumen. (*C, F,* and *I*) *Mthfdl1* gene expression visualized by in situ hybridization in a whole mount embryo (*C*) and a section through the same embryo (*F* and *I*). Precise age of embryos: A, 37 somites; B, 34 somites; C, 33 somites; J, 44 somites; and K, 42 somites. The regions outlined by dashed boxes are magnified in the panels immediately below them. (Magnification: *A–C*,1.6×; *J* and *K*, 1.25×.) Black arrowheads in *D*, *E*, *F*, *L*, and *M* highlight areas of β-galactosidase staining or in situ hybridization.

displayed normal neural tube closure and 3 had exencephaly (Fig. 5 *B* and *D*). Thus, compared with nulls from unsupplemented dams, formate supplementation at 7,500 mg·kg^{-1}·d^{-1} gives a significantly higher frequency of nulls with normal neural tube closure ($P = 0.028$). Importantly, 6 of the 14 *Mthfd1l*$^{z/z}$ embryos were dissected from dams at E13.5 or E15.5, whereas no surviving *Mthfd1l*$^{z/z}$ embryos were observed after E12.5 from unsupplemented dams. Although we could not compare supplemented versus nonsupplemented embryos after E12.5 because of lethality of the unsupplemented embryos, formate supplementation partially rescues the growth defect in *Mthfd1l*$^{z/z}$ embryos (Fig. 5 *A* and *B*). The crown–rump length of formate supplemented *Mthfd1l*$^{z/z}$ E11.5 embryos was significantly greater than in unsupplemented *Mthfd1l*$^{z/z}$ embryos (5.0 ± 0.1 vs. 3.6 ± 0.3 mm, respectively; $P < 0.01$). Supplementation had no significant effect on crown–rump length of WT embryos (5.9 ± 0.2 mm).

Discussion

In this study, we have shown that all embryos lacking *Mthfd1l* exhibit aberrant neural tube closure including craniorachischisis and exencephaly and/or a wavy neural tube. The NTD phenotype (exencephaly and craniorachischisis) is accompanied by abnormal neural tube morphology characterized by asymmetric bulges in the neuroepithelium and a wider lumen in wavy areas of the neural tube. In addition to the NTD phenotype, *Mthfd1l*$^{z/z}$ embryos show immature maxillary and mandibular process development. Finally, we show that maternal formate supplementation significantly reduces the incidence of NTDs, partially rescues the growth defect, and allows survival past the point of lethality seen in unsupplemented *Mthfd1l*$^{z/z}$ embryos. This knockout mouse is a fully penetrant folate-pathway mouse model that does not require feeding a folate-deficient diet to cause these phenotypes. More than 10 folate-related mouse mutants have been characterized thus far (16), but NTDs are observed in only three: *Folr1, Shmt1*, and *Amt*. *Folr1* encodes folate receptor 1, one of the major folate transport systems, and homozygous knockout of *Folr1* produces a severe folate deficiency in the embryo that can be rescued with maternal 5-formyl-THF supplementation (17). This rescue is "tunable," and depending on the dose of 5-formyl-THF administered to mothers during

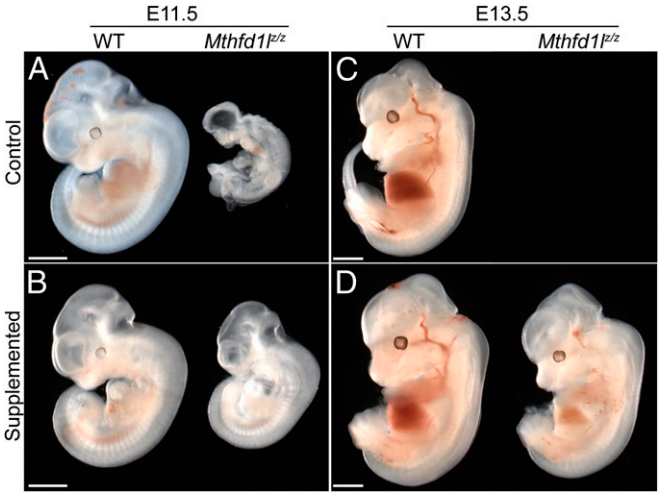

Fig. 5. Maternal supplementation with sodium formate improves development and growth in *Mthfd1l*$^{z/z}$ embryos. Pregnant dams were administered a calculated dose of 7,500 mg·kg^{-1}·d^{-1} sodium formate. *Mthfd1l*$^{z/z}$ embryos dissected at E11.5 (*B*) Improved growth compared with control embryos from unsupplemented dams (*A*). E13.5 embryos from unsupplemented (*C*) and supplemented (*D*) dams. Precise age of embryos: (*A*) WT, 47 somites; z/z, 36 somites; (*B*) WT 45 somites; and z/z, 41 somites; (*D*) not determined because tails were not intact. (Scale bars, 1.0 mm.)

gestation, *Folr1*$^{-/-}$ embryos develop NTDs and orofacial deformities or can be rescued to birth. Homozygous knockout of *Shmt1*, which encodes a cytoplasmic folate-metabolizing enzyme (Fig. 1, reaction 4), gives rise to a low frequency of NTDs in embryos from *Shmt1*$^{-/-}$ dams fed a folate-deficient diet (18, 19). *Amt* encodes an aminomethyltransferase that is a subunit of the mitochondrially localized glycine cleavage system (GCS), which processes glycine to donate 1C units to THF, forming CH_2-THF (Fig. 1, reaction 5). Homozygous deletion of *Amt* is embryonically lethal, and *Amt*$^{-/-}$ embryos develop NTDs with 87% penetrance (20). The phenotype exhibited by the *Amt* knockout mouse suggests that the demand for 1C units is high during neurulation. This is consistent with the observation that maternal supplementation with methionine, which provides 1C units via the methyl cycle (Fig. 1), significantly improves neurulation in *Amt* null embryos, whereas folic acid has no effect (20). The importance of the GCS to neural tube development is also supported by the occurrence of NTDs in the *nehe* mouse (21). The *nehe* mouse carries a hypomorphic allele of lipoic acid synthetase, the mitochondrial enzyme that catalyzes the synthesis of lipoic acid, an essential cofactor for GCS and several other mitochondrial enzymes. One other folate pathway mouse model, targeting *Mthfd1* (Fig. 1, cytoplasmic reactions 1–3), also displays disorganized neural tube closure in heterozygous *Mthfd1*$^{gt/+}$ embryos from *Mthfd1*$^{gt/+}$ dams fed a folate-deficient diet (22). Although the defects in this model are not classic NTDs, they are reminiscent of the wavy neural tube phenotype we observe in *Mthfd1l*$^{z/z}$ embryos.

Our observation that *Mthfd1l*$^{z/z}$ embryos develop NTDs confirms that integrity of the mitochondrial 1C pathway is essential for normal neural tube development. As illustrated in Fig. 1, mitochondria possess multiple enzymes that produce CH_2-THF from various 1C donors (reactions 4m, 5, 8, and 9) (4). Embryonic mitochondria also possess redundant dehydrogenase/cyclohydrolase enzymes that can oxidize CH_2-THF to 10-CHO-THF (MTHFD2 and MTHFD2L; reactions 2m and 3m). MTHFD2 is expressed in transformed cells and embryonic or nondifferentiated tissues, but not in adult differentiated tissues (23). Homozygous knockout of *Mthfd2* is embryonic lethal, but does not cause NTDs (24). *Mthfd2* nullizygous embryos develop to about E15.5 and display no gross developmental abnormalities, but they are noticeably smaller and paler than WT and heterozygous littermates. The lack of NTDs in *Mthfd2* nullizygous embryos is likely due to the existence of MTHFD2L, a second mitochondrial dehydrogenase/cyclohydrolase. MTHFD2L is expressed in embryos and adults (8) and can presumably support mitochondrial 1C flux to the level of 10-formyl-THF in *Mthfd2* nullizygous embryos.

On the other hand, only one enzyme with 10-formyl-THF synthetase activity (MTHFD1L) is known to exist in mitochondria, and this activity is required to produce formate and THF from 10-CHO-THF (Fig. 1, reaction 1m). Thus, loss of MTHFD1L activity is expected to completely abolish mitochondrial formate production. This metabolic block would then starve the cytoplasm for formate, creating a "formyl trap", analogous to the methyl trap seen when 5-methyl-THF accumulates in vitamin B_{12}-deficient cells (25, *). Although the *Mthfd1l* knockout mouse is replete of folate, it has no way to catalyze the conversion of 10-formyl-THF to THF plus formate, leading to a trapping of mitochondrial 1C units as 10-formyl-THF, which cannot exit the mitochondrion. This in turn would cause a deficiency in cytoplasmic 1C units, which are needed in stoichiometric amounts for purine and thymidylate production as well as the methyl cycle. The phenotypes of the *Shmt1* and *Amt* knockout mice are consistent with this model of mammalian 1C metabolism. The *Shmt1* gene, which encodes cytoplasmic serine hydroxymethyltransferase (Fig. 1, cytoplasmic reaction 4), is not essential in mice (26), indicating that mitochondrial SHMT (mitochondrial reaction 4m) is fully capable of providing all of the 1C units needed in both the embryo and the adult. The neural tube phenotype in *Amt* nullizygous embryos lacking GCS activity (mitochondrial reaction 5) (20) is less severe than that in *Mthfd1l* knockout embryos. Presumably, the existence of alternative mitochondrial 1C donors (e.g., serine) allows some of the *Amt*$^{-/-}$ embryos to develop normally. On the other hand, *all* mitochondrial 1C units, whatever their source, must pass through the MTHFD1L reaction to supply the cytoplasm with formate; any defect in this step would be expected to cause a more severe phenotype. The importance of mitochondrially derived formate is supported by our results demonstrating a significant reduction in the incidence of NTDs and partial rescue of *Mthfd1l*$^{z/z}$ embryonic growth with maternal formate supplementation.

MTHFD1L thus controls the flux of 1C units from mitochondria into cytoplasmic processes such as purine and thymidylate biosynthesis and the methyl cycle (Fig. 1). De novo purine biosynthesis is essential for cell division, and *S*-adenosylmethionine synthesis is critical for chromatin and DNA methylation, which play essential roles during cell differentiation (27, 28) and cell migration (29). Epigenetic modifications are particularly dynamic, with extensive reprogramming of DNA methylation during early embryogenesis (30). Disruption of the methyl cycle is known to induce NTDs in cultured mouse embryos (31) and cranial defects are observed in DNA methyltransferase 3b nullizygous embryos (32). Recent studies in humans have linked maternal folate status and occurrence of NTDs to tissue-specific DNA hypo- and hypermethylation patterns, with decreased DNA methylation observed in NTD brain tissue compared with normal embryos (33). Protein methylation is also involved in neural tube development, and hypomethylation of neural tube proteins is accompanied by a failure of the neural tube to close in rat embryos cultured in methionine-deficient conditions (34). The cytoskeletal proteins β-actin and tubulin are known to be methylated during neural tube closure (35), and proper function of the cytoskeleton is required for cranial neural tube closure (reviewed in ref. 36).

A common polymorphism in *MTHFD1L* has been shown to be strongly associated with NTD risk in an Irish population (13), suggesting that MTHFD1L also plays an important role in human neural tube development. Importantly, disruption of MTHFD1L function does not cause cellular folate deficiency (like a transport defect); rather, it blocks a specific metabolic step: the production and release of formate from mitochondria into the cytoplasm. This metabolic defect causes aberrant neural tube closure including craniorachischisis and exencephaly and/or a wavy neural tube phenotype in 100% of *Mthfd1l*$^{z/z}$ embryos (Fig. 3). The *Mthfd1l* mouse model should prove useful for identifying the mechanisms that underlie the folate dependence of normal neural tube development as well as for defining the metabolic pathways that are most severely affected by cytoplasmic formate deficiency. Determination of these pathways will enhance our understanding of folate-mediated 1C metabolism and may even suggest additional interventions to protect against folate-resistant NTDs in humans.

Methods

Mice. All protocols used within this study were approved by the Institutional Animal Care and Use Committee of The University of Texas at Austin and conform to the National Institutes of Health Guide for the Care and Use of Laboratory Animals. All mice were maintained on a C57BL/6 genetic background. Mice harboring a floxed conditional knockout cassette between exons 4 and 6 of *Mthfd1l* were obtained from the Wellcome Trust Sanger Institute (EUCOMM ID 37226). Mice carrying the floxed *Mthfd1l* allele were mated to mice expressing Cre recombinase under control of the *E2a* promoter (E2a-Cre) (14) to generate heterozygous *Mthfd1l*$^{z/+}$ embryos lacking exon 5 and the neomycin resistance cassette (Fig. 2*A*). All mice were given ad libitum access to water and standard mouse chow (LabDiet 5K67).

Genotyping. Genotyping was carried out by a modified PCR method (37). A mixture of three primers was used to detect the WT and/or recombined allele (Fig. 2*A*). To detect the WT allele, a forward primer (F) binding in the 5′

*Noronha JM, Silverman M (1962) On folic acid, vitamin B12, methionine and formiminoglutamic acid metabolism. Vitamin B12 and Intrinsic Factor, Second European Symposium, ed Heinrich HC (Verlag, Stuttgart), pp 728–736.

region outside of the conditional cassette (5′-GAGTATGTGATTGCTTG-GACCCCCAGGTTCC-3′) and a reverse primer (R1) binding 5′ to exon 5 (5′-TGGCTCCCGAGGTTGTCTTCTGGCTATGAT-3′) were used. Amplification using these primers results in a 444-bp amplicon from the WT allele. Amplification of the mutant allele uses the forward primer F and a reverse primer (R2) complementary to a region only found in the gene-targeting cassette (5′-CGGCGCCAGCCTGCTTTTTTGTACAAACTTG-3′). Amplification using these primers results in a 324-bp amplicon in the presence of the mutant allele. See Fig. 2*A* for a schematic of primer binding sites used to detect *Mthfd1l* and *Mthfd1l*^{z}. Cre recombinase was detected using 5′-GCATTACCGGTC-GATGCAACGAGTGATGAG-3′ and 5′-GAGTGAACGAACCTGGTCGAAATCAG-TGCG-3′ to produce a 408-bp amplicon, and SRY was detected using 5′-TTGTCTAGAGAGCATGGAGGGCCATGTCAA-3′ and 5′-CCACTCCTCTGTGACA-CTTTAGCCCTCCGA-3′ to detect a 273-bp amplicon.

RT-PCR. Total RNA was prepared from *Mthfd1l*$^{+/+}$, *Mthfd1l*$^{z/+}$, and *Mthfd1l*$^{z/z}$ mouse embryos dissected at E11.5. First-strand cDNA was synthesized using the SuperScript III First-Strand Synthesis System (Invitrogen) and random hexamers. PCR was performed using a forward primer f (5-CTCACATCT-GCTTGCCTCCA-3′) binding in exon 4 and a reverse primer r (5′-ATGTCCC-CAGTCAGGTGAAG-3′) binding in exon 14 to amplify a 1,087-bp amplicon from the WT transcript (see Fig. 2*A* for a schematic of primer binding sites). Primers amplifying a 115-bp amplicon (forward: 5′-AGAGACGGCCGCAT-CTTC-3′, reverse: 5′-CAAATGGCAGCCCTGGTGA-3′) from GAPDH were used as a positive control for cDNA quality.

Mitochondrial Isolation and Immunoblotting. Mitochondria were isolated from one embryo (*Mthfd1l*$^{+/+}$ and *Mthfd1l*$^{z/+}$) or three embryos (*Mthfd1l*$^{z/z}$) as previously described (12), except embryos were homogenized by pipetting. Protein concentration was determined by BCA assay (Thermo Fisher Scientific). Proteins were separated by SDS/PAGE and immunoblotted using rabbit polyclonal anti-MTHFD1L (1:1,000) (11). After incubation with HRP-conjugated goat anti-rabbit IgG (1:5,000) (Invitrogen), reacting bands were detected using ECL Plus (GE Healthcare Life Sciences). After stripping, blots were reprobed with rabbit polyclonal anti-Hsp60 (1:1,000) (Enzo Life Sciences).

Histology. Embryos were stained for β-galactosidase activity overnight as described previously (38). Stained embryos were embedded in paraffin, sectioned at the level of the forelimb (4-μm thickness) and counterstained with nuclear fast red. *Mthfd1l* whole mount in situ hybridization was performed using a riboprobe against the 3′ UTR as previously described (12). Embryos were then embedded in OCT medium and cryosectioned at the level of the forelimb (12-μm thickness).

Maternal Supplementation with Sodium Formate. *Mthfd1l*$^{z/+}$ matings were set up in a cage equipped with a water bottle containing either 0.37M or 0.55M sodium formate. The females had access to the supplemented water at least 1 d before observation of the plug. These concentrations were calculated to deliver either 5,000 or 7,500 mg sodium formate·kg^{-1}·d^{-1}, respectively, based on an average water intake of 5 mL/d for a 25-g C57BL/6 mouse (39). The effect of formate supplementation was analyzed by a two-sided χ^2 test for NTD incidence and two-way ANOVA with Bonferroni posttest for crown–rump length.

ACKNOWLEDGMENTS. We thank Dr. Jacqueline Tabler for observational insights. This work was supported by National Institutes of Health Grant GM086856 (to D.R.A.) and by startup funds from the College of Natural Sciences and the Institute for Cellular and Molecular Biology at the University of Texas at Austin (to S.A.V.).

1. Hibbard ED, Smithells RW (1965) Folic acid metabolism and human embryopathy. *Lancet* 1(7398):1254.
2. Ross ME (2010) Gene-environment interactions, folate metabolism and the embryonic nervous system. *Wiley Interdiscip Rev Syst Biol Med* 2(4):471–480.
3. Hobbs CA, Shaw GM, Werler MM, Mosley B (2010) Folate status and birth defect risk. Epidemiological perspective. *Folate in Health and Disease*, ed Bailey LB (CRC Press, Taylor & Francis Group, Boca Raton, FL), 2nd ed, pp 133–153.
4. Tibbetts AS, Appling DR (2010) Compartmentalization of mammalian folate-mediated one-carbon metabolism. *Annu Rev Nutr* 30:57–81.
5. Mejia NR, MacKenzie RE (1988) NAD-dependent methylenetetrahydrofolate dehydrogenase-methenyltetrahydrofolate cyclohydrolase in transformed cells is a mitochondrial enzyme. *Biochem Biophys Res Commun* 155(1):1–6.
6. Mejia NR, MacKenzie RE (1985) NAD-dependent methylenetetrahydrofolate dehydrogenase is expressed by immortal cells. *J Biol Chem* 260(27):14616–14620.
7. Barlowe CK, Appling DR (1988) In vitro evidence for the involvement of mitochondrial folate metabolism in the supply of cytoplasmic one-carbon units. *Biofactors* 1(2): 171–176.
8. Bolusani S, et al. (2011) Mammalian MTHFD2L encodes a mitochondrial methylenetetrahydrofolate dehydrogenase isozyme expressed in adult tissues. *J Biol Chem* 286(7):5166–5174.
9. Prasannan P, Pike S, Peng K, Shane B, Appling DR (2003) Human mitochondrial C1-tetrahydrofolate synthase: Gene structure, tissue distribution of the mRNA, and immunolocalization in Chinese hamster ovary calls. *J Biol Chem* 278(44):43178–43187.
10. Walkup AS, Appling DR (2005) Enzymatic characterization of human mitochondrial C1-tetrahydrofolate synthase. *Arch Biochem Biophys* 442(2):196–205.
11. Prasannan P, Appling DR (2009) Human mitochondrial C1-tetrahydrofolate synthase: Submitochondrial localization of the full-length enzyme and characterization of a short isoform. *Arch Biochem Biophys* 481(1):86–93.
12. Pike ST, Rajendra R, Artzt K, Appling DR (2010) Mitochondrial C1-tetrahydrofolate synthase (MTHFD1L) supports the flow of mitochondrial one-carbon units into the methyl cycle in embryos. *J Biol Chem* 285(7):4612–4620.
13. Parle-McDermott A, et al. (2009) A common variant in MTHFD1L is associated with neural tube defects and mRNA splicing efficiency. *Hum Mutat* 30(12):1650–1656.
14. Lakso M, et al. (1996) Efficient in vivo manipulation of mouse genomic sequences at the zygote stage. *Proc Natl Acad Sci USA* 93(12):5860–5865.
15. Harris MJ, Juriloff DM (2007) Mouse mutants with neural tube closure defects and their role in understanding human neural tube defects. *Birth Defects Res A Clin Mol Teratol* 79(3):187–210.
16. Harris MJ, Juriloff DM (2010) An update to the list of mouse mutants with neural tube closure defects and advances toward a complete genetic perspective of neural tube closure. *Birth Defects Res A Clin Mol Teratol* 88(8):653–669.
17. Spiegelstein O, et al. (2004) Embryonic development of folate binding protein-1 (Folbp1) knockout mice: Effects of the chemical form, dose, and timing of maternal folate supplementation. *Dev Dyn* 231(1):221–231.
18. Beaudin AE, et al. (2011) Shmt1 and de novo thymidylate biosynthesis underlie folate-responsive neural tube defects in mice. *Am J Clin Nutr* 93(4):789–798.
19. Beaudin AE, et al. (2012) Dietary folate, but not choline, modifies neural tube defect risk in Shmt1 knockout mice. *Am J Clin Nutr* 95(1):109–114.
20. Narisawa A, et al. (2012) Mutations in genes encoding the glycine cleavage system predispose to neural tube defects in mice and humans. *Hum Mol Genet* 21(7):1496–1503.
21. Zhou X, Anderson KV (2010) Development of head organizer of the mouse embryo depends on a high level of mitochondrial metabolism. *Dev Biol* 344(1):185–195.
22. Beaudin AE, Perry CA, Stabler SP, Allen RH, Stover PJ (2012) Maternal Mthfd1 disruption impairs fetal growth but does not cause neural tube defects in mice. *Am J Clin Nutr* 95(4):882–891.
23. Christensen KE, Mackenzie RE (2008) Mitochondrial methylenetetrahydrofolate dehydrogenase, methenyltetrahydrofolate cyclohydrolase, and formyltetrahydrofolate synthetases. *Vitam Horm* 79:393–410.
24. Di Pietro E, Sirois J, Tremblay ML, MacKenzie RE (2002) Mitochondrial NAD-dependent methylenetetrahydrofolate dehydrogenase-methenyltetrahydrofolate cyclohydrolase is essential for embryonic development. *Mol Cell Biol* 22(12):4158–4166.
25. Herbert V, Zalusky R (1962) Interrelations of vitamin B12 and folic acid metabolism: folic acid clearance studies. *J Clin Invest* 41:1263–1276.
26. MacFarlane AJ, et al. (2008) Cytoplasmic serine hydroxymethyltransferase regulates the metabolic partitioning of methylenetetrahydrofolate but is not essential in mice. *J Biol Chem* 283(38):25846–25853.
27. Bai S, et al. (2005) DNA methyltransferase 3b regulates nerve growth factor-induced differentiation of PC12 cells by recruiting histone deacetylase 2. *Mol Cell Biol* 25(2):751–766.
28. Kobayakawa S, Miike K, Nakao M, Abe K (2007) Dynamic changes in the epigenomic state and nuclear organization of differentiating mouse embryonic stem cells. *Genes Cells* 12(4):447–460.
29. Horswill MA, Narayan M, Warejcka DJ, Cirillo LA, Twining SS (2008) Epigenetic silencing of maspin expression occurs early in the conversion of keratocytes to fibroblasts. *Exp Eye Res* 86(4):586–600.
30. Borgel J, et al. (2010) Targets and dynamics of promoter DNA methylation during early mouse development. *Nat Genet* 42(12):1093–1100.
31. Dunlevy LP, et al. (2006) Integrity of the methylation cycle is essential for mammalian neural tube closure. *Birth Defects Res A Clin Mol Teratol* 76(7):544–552.
32. Okano M, Bell DW, Haber DA, Li E (1999) DNA methyltransferases Dnmt3a and Dnmt3b are essential for de novo methylation and mammalian development. *Cell* 99(3):247–257.
33. Chang H, et al. (2011) Tissue-specific distribution of aberrant DNA methylation associated with maternal low-folate status in human neural tube defects. *J Nutr Biochem* 22(12):1172–1177.
34. Coelho CN, Klein NW (1990) Methionine and neural tube closure in cultured rat embryos: morphological and biochemical analyses. *Teratology* 42(4):437–451.
35. Moephuli SR, Klein NW, Baldwin MT, Krider HM (1997) Effects of methionine on the cytoplasmic distribution of actin and tubulin during neural tube closure in rat embryos. *Proc Natl Acad Sci USA* 94(2):543–548.
36. Copp AJ, Greene ND, Murdoch JN (2003) The genetic basis of mammalian neurulation. *Nat Rev Genet* 4(10):784–793.
37. Stratman JL, Barnes WM, Simon TC (2003) Universal PCR genotyping assay that achieves single copy sensitivity with any primer pair. *Transgenic Res* 12(4):521–522.
38. Whiting J, et al. (1991) Multiple spatially specific enhancers are required to reconstruct the pattern of Hox-2.6 gene expression. *Genes Dev* 5(11):2048–2059.
39. Green EL, ed (1966) *Biology of the Laboratory Mouse* (Dover Publications, Inc., New York), 2nd ed, p 706.